Int. J. Chem. Sci.: 14(2), 2016, 671-682
ISSN 0972-768X
www.sadgurupublications.com

STRUCTURAL AND OPTICAL PROPERTIES OF ZINC TITANATE ELECTROSPUN ONE DIMENSIONAL NANOSTRUCTURES

ACHRAF HAMROUNI[*,a,b], ABDELAZIZ DRICI[a], PHILIPPE MIELE[c], RAOUIA HAMROUNI[a] and ABDELAZIZ AMARA[a]

[a]Study and Research of Condensed Statements Laboratory (LEREC), Badji Mokhtar University, Annaba- B.P.12, ANNABA 23000, ALGERIA
[b]Inorganic Materials Chemistry Laboratory (LCMI), Badji Mokhtar University, Annaba- B.P.12, ANNABA 23000, ALGERIA
[c]European Institute of Membranes, UMR 5635 CNRS ENSCM University Montpellier, Place Eugene Bataillon, F-34095 MONTPELLIER CEDEX 5, FRANCE

ABSTRACT

This paper reports the synthesis and the characterization of 1D Zinc titanate nanobelts of different molar ratios Zn/Ti = 0.26-0.40-0.80 ($Zn(CH_3COO)_2$/TTIP) prepared by electrospinning. The samples were annealed at 600°C and 900°C temperatures in air for 5 hr. The as-spun and annealed ($Zn(CH_3COO)_2$/ TTIP)/PVP composite nanobelts were characterized by scanning electron microscopy (SEM), Energy-dispersive X-ray spectroscopy analysis (EDX), X-ray diffraction (XRD), Raman spectroscopy and photoluminescence (PL). The results in this paper demonstrate that heat treatment has an influence on the process of crystallization. According to the X-ray diffraction, the formation of $ZnTiO_3$ rhombohedral phase. Raman spectroscopy results confirm the formation of $ZnTiO_3$ phase. They are in good agreement with the X-ray diffraction. Photoluminescence reveals that high quantity of Titanium makes shift from emitted bands to greater wavelengths (visible region). However, high temperature causes a shift from emission bands to greater wavelengths and regeneration of other bands.

Key words: Titanium oxide, Zinc oxide, Electrospinning, 1D, Nanobelts, Photoluminescence.

INTRODUCTION

Tansparent conductive oxides (TCO) such as Zinc oxide (ZnO) and titanium oxide (TiO_2) have attracted considerable attention in different fields such as photovoltaic[1,2] optoelectronics[3], touch screens[4], electrochromic devices[5] and flat panel displays[6-8] and due

[*]Author for correspondence; E-mail: achraf_hamrouni58@yahoo.fr

to their transparency to visible light and good conductivity[9]. The elaboration of such materials at nanoscale such as one-dimensional nanostrcutures[10-13] have attracted many researchers because of their outstanding physical and chemical properties.

Different synthetic strategies have been elaborated to design these 1D nanostructures like high temperature physical evaporation[14], template-directed methods[15], electrospinning[16], solvothermal synthesis[17] and self-assembly methods. These materials were obtained in different shapes like nanotubes, nanofibers[18,19], nanowires[20] and anocables. Among these synthesis techniques, the electrospinning is a simple and low cost method[21] that allows manufacturing 1D nanomaterials with an easy control of the chemical and physical properties[22].

Since 1960s many researchers have been interested in Zinc titanate ($ZnTiO_3$) materials and its characterizations. It has three crystalline phases: $ZnTiO_4$ (CFC), $ZnTio_3$ (hexagonal) and $Zn_2Ti_3O_8$ (cubic), and undergoes many transformations at different temperatures. At a temperature, superior than about 800°C, $ZnTi_3O_8$ is decomposed into $ZnTiO_3$ and rutile TiO_2 phase. At about 945°C, $ZnTiO_3$ is decomposed into Zn_2TiO_4, while TiO_2 rutile is a stable phase and an important photocatalytic material[16].

In this paper, we have fabricated $ZnTiO_3$ nanobelts by electrospinning method and detailed structural and optical characterization of the obtained nanostructures. The structural and optical changes induced by high temperature annealing will be discussed here. The photoluminescence properties of these nanomaterials will be also highlighted.

EXPERIMENTAL

Titanium tetra-isopropoxide TTIP ($Ti\{OCH(CH_3)_2\}_4$; 97%,), zinc acetate ($Zn(CH_3COO)_2$ 99.99%), polyvinyl pyrrolidone PVP (Mw = 1300000), ethanol (98%) and dimethyl-formamide (DMF, 99.8%) were purchased from Sigma–Aldrich.

Zinc titanate 1D nanostructures were synthesized by electrospinning technique using titanium tetra-isopropoxide (TTIP) and zinc acetate $Zn(CH_3COO)_2$ as precursors. In a typical experiment three solutions were prepared of three different ratio molars Zn/Ti= 0.26-0.40 and 0.80. 0.25 g of zinc acetate $Zn(CH_3COO)_2$ was dissolved in a mixture of 5 mL DMF, 2.5 mL ethanol and 5 g of PVP was added then to the solution. The ratio molar of the latter is Zn/Ti = 0.26. The Zn/Ti = 0.40 and 0.80 was prepared with the same method by changing the volume of TTIP and adding 1 and 1.5 mL, respectively. The precursor mixtures were

stirred for 15 min at room temperature to obtain sufficient viscosity required for electrospinning. The electrospinning solutions were placed into a 22 mL syringe with a 25 gauge stainless steel needle at the tip. The syringe pump was adjusted to 0.3 mL/hr of feeding rate. Then, the electric voltage of 30 kv was applied between the needle and the collector. The distance between the tip of the syringe needle and the collector (Al plate) was fixed to 17 cm. The samples were left overnight in air to fully hydrolyze. To remove the polymer and achieve crystallinity, the composite were then treated in air at different temperatures 600^{o}C, and 900^{o}C for 5 hr with a heating rate of 2°C/min. The microstructures, the phase and the crystal structure of the 1D nanostructures synthesized were analysed using scanning electron microscopy (SEM, Hitachi S-4800), X-ray diffraction (Panalyticalxpert-PRO diffractometer equipped with ax'celerator detector using Ni-filtered Cu-radiation), Raman (Jobin-Yvon S. A., Horiba, France) and Energy-dispersive X-ray spectroscopy analysis (Zeiss EVO ED15 microscope coupled with an Oxford X-maxn EDX detector). Photoluminescence of 1D nanostructures was measured at room temperature using the experimental setup, described elsewhere by Chaaya et al.[23] The PL was excited by solid state laser (355 nm) and the emission spectra were recorded in the range 360-800 nm.

RESULTS AND DISCUSSION

The morphology of the obtained 1D nanostructures was examined by scanning electron microscopy (SEM). The composite obtained were treated in air at different temperatures: 600^{o}C Fig. 1 (a-c) and 900^{o}C Fig. 1 (d-f). As shown in Fig. 1 (a-c), the 1D NSs exhibit at 600^{o}C a nanobelt like structures with an average thickness of 120 nm and width of 800 nm. After calcination at 900^{o}C Fig. 1 (d-f), the average thickness and width decreases to 90 nm and 600 nm, respectively. This can be explained by the process of crystallization. The loss of ethanol and DMF, the degradation of PVP and the decomposition of TTIP[24].

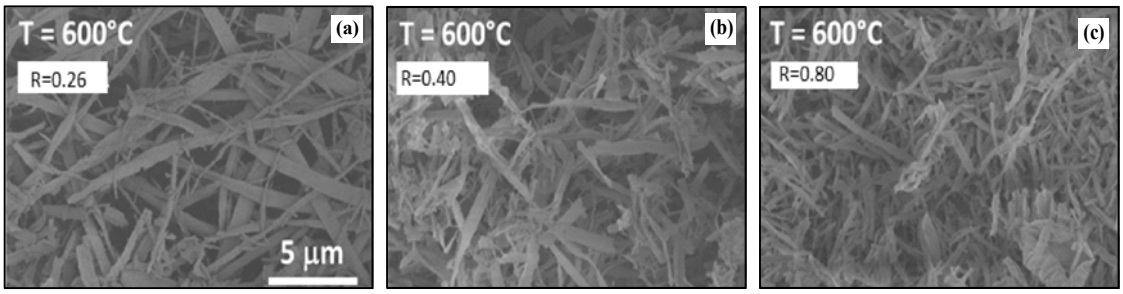

Cont…

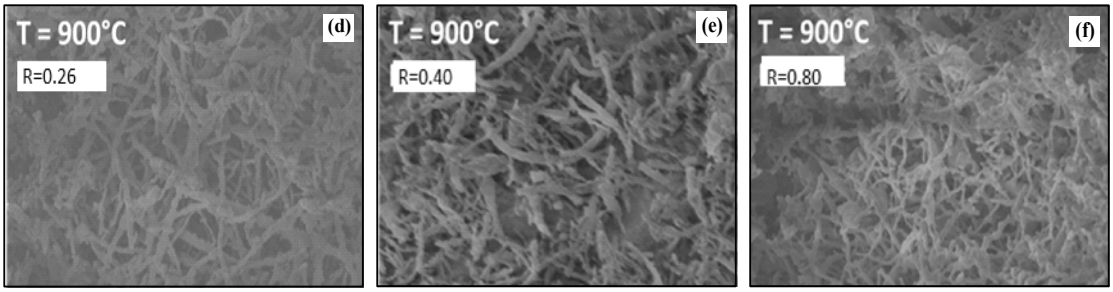

Fig. 1: Scanning electron microscopy images of the 1D nanostructures with different Zn/Ti molar ratios annealed in air at various temperatures for 5h: 600°C (a-c) and 900°C (d-f)

EDS analysis shown in Table 1 reveals the presence of Ti, Zn and O. No other elements are present in the sample. This confirms that heat treatment at 600°C and 900°C removes PVP, DMF and ethanol completely from the nanobetls. The X-ray diffraction indicates the formation of zinc titanate oxide $ZnTiO_3$ rhombohedrique for different ratio molars at 600°C and 900°C. At 600°C Fig. 2(a) and for different ratio molars, there is a formation of $ZnTiO_3$ phase; i. e. the variation of ratio molar does not influence on the formation of $ZnTiO_3$ phase. Group space is G.S: R3 (148), lattice parameters a = b = c = 5.07 and angle $\alpha = \beta = \gamma \neq 90°$. It is justified by the presence of the most intense peaks (104) and (110) were observed at $2\theta = 32.84°$ and $2\theta = 35.20°$, respectively, while the weak peaks at 23.82°, 40.29°, 41.14°, 48.76°, 53.34°, 56.69°, 61.73°, 63.25° and 68.89° correspond to (012), (113), (021), (024), (116), (018), (214), (300) and (112), respectively. This results are in good agreement with what is reported in the map data JCPDS [26-1500]. This formation is due to the reaction between zinc oxide and titanium oxide obtained by the decomposition of organometallic precursors at 345°C[16]. However, $ZnTiO_3$ starts to crystalize at 450°C[16]. The appearance of pics ZnO hexagonal phase[25] and TiO_2 rutile-anatase phases[25] with different proportions is due to variation of molar ratio between the samples. Appearance of Zn_2TiO_4 cubic phase when Zn/Ti = 0.4 and in existence when Zn/Ti = 0.26 and 0.8, which is justified by the effect of the amount of Ti, which was different to Zangying et al. report. In the report of Zangying et al. is mentioned temperature less than 885°C. $ZnTiO_3$ exists and decomposes at temperature more than 900°C to Zn_2TiO_4 and TiO_2 rutile, which are different from our results is due to time of calcination chosen and the amount of Titanium because there is no formation of Zn_2TiO_4 at 600°C after 1.5 hr of calcinations[16]. At 900°C Fig. 2(b), complete formation of $ZnTiO_3$ rhombohedral phase, transformation of TiO_2 anatase to TiO_2 rutile, there is a ZnO trace and TiO_2 anatase. In existence of Zn_2TiO_4 phase after calcination

is different to Zanying report, which is different of our results. The absence $Zn_2Ti_3O_8$ phase is similar to Zanying et al.[16] report and different to How[26].

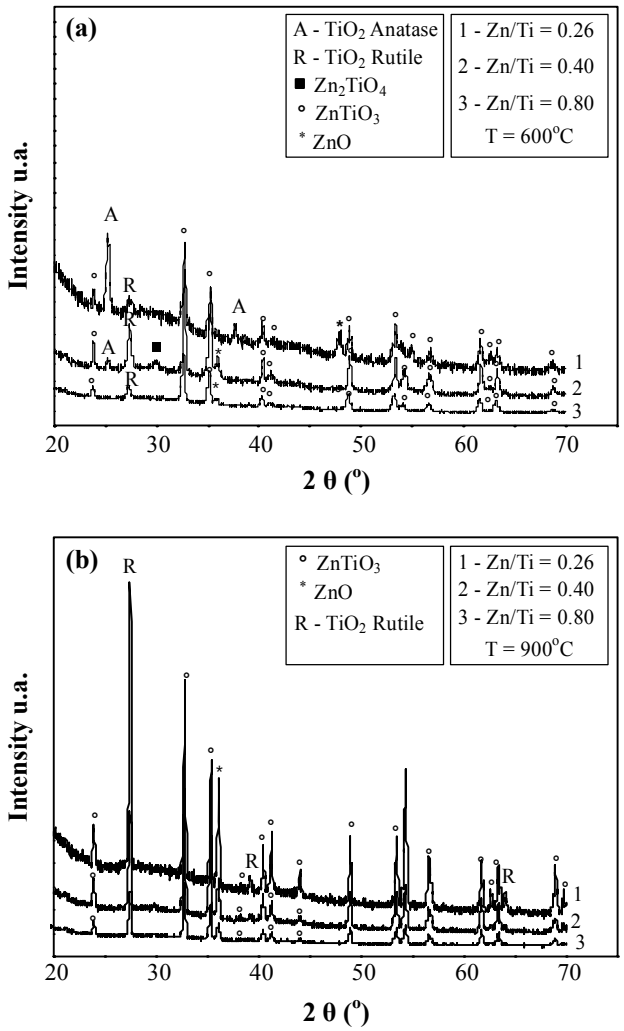

Fig. 2: (a) XRD patterns of different molar ratios zinc titanate $ZnTiO_3$ nanobelts annealed at 600°C in air for 5h. (b) XRD patterns of different molar ratios zinc titanate $ZnTiO_3$ nanobelts annealed at 900°C in air for 5h

Raman spectroscopy was performed for examining the formation of phase and the vibrational modes. The $ZnTiO_3$ nanobelts synthesized by different ratio molars and calcined at 600°C and 900°C were examined by Raman spectroscopy. The spectra were taken at room temperature using a 532 nm laser line as the excitation source. This technique has been able

to demonstrate the formation of $ZnTiO_3$ Rhomboedral phase. Fig. 3(a-b) shows Raman spectra of the $ZnTiO_3$ nanobelt calcined at 600°C, and 900°C. At 600°C [Fig. 3(a)] when Zn/Ti = 0.26 $ZnTiO_3$ rhomboedral structure is identified by four Raman bands at (177-231-266-709) cm^{-1}. The position of bands of $ZnTiO_3$ as shown Fig. 3(a) are approximately in good agreement with the X-ray diffraction[28].

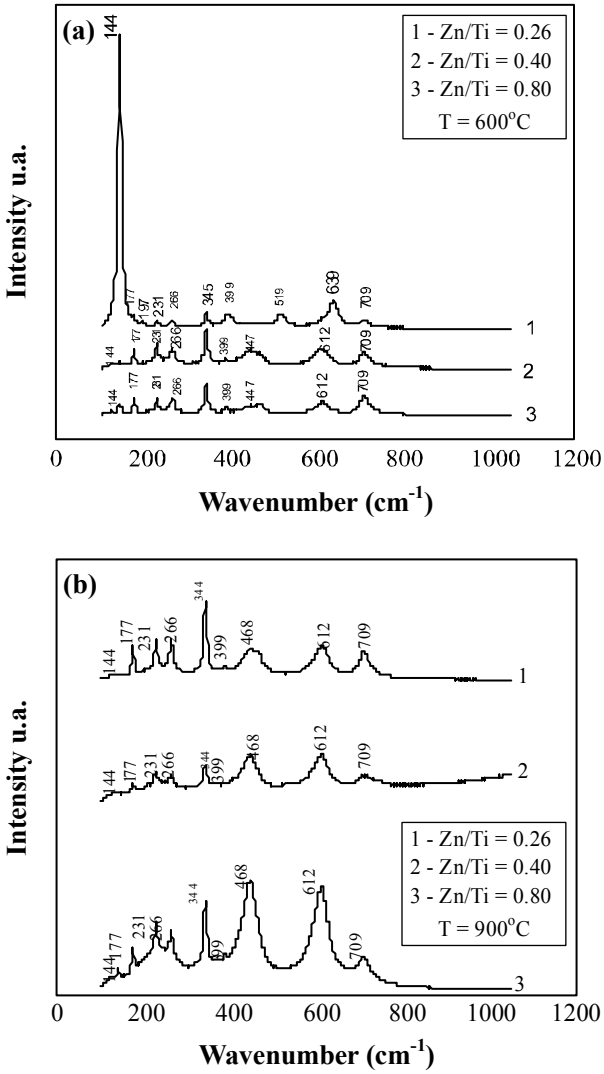

Fig. 3: (a) Raman spectra of $ZnTiO_3$ nanobelts of different molar ratios annealed at 600°C in air for 5h. (b) Raman spectra of $ZnTiO_3$ nanobelts of different molars ratios annealed at 900°C in air for 5h

The bands (144 (E_g)-197(E_g)-399 (B_{1g})-519 (B_{1g})-639 (A_1 + B_{1g}) represent the vibrational modes, which are active in spectroscopy of anatase phase of TiO_2.[28-32]

Table 1: EDX data showing the weight percent of elements of $ZnTiO_3$ annealed at 600 and 900°C

	600°C			900°C		
	R = 0.26	**R = 0.40**	**R = 0.80**	**R = 0.26**	**R = 0.40**	**R = 0.80**
Zn	07.22	10.29	14.40	06.86	09.13	13.46
Ti	27.15	25.33	18.22	28.43	26.74	19.16
o	65.63	66.02	68.38	64.71	64.10	67.38

The band at 144 cm^{-1} appear with a higher in intensity. The band at 345 cm^{-1} identify ZnO Wurtsite structure (multiple-phonon scattering processes)[27]. When Zn/Ti = 0.4 and 0.80 $ZnTiO_3$ rhomboedral structure is identified by four raman bands at (177-231-266-709) cm^{-1} The position of bands of $ZnTiO_3$ as shown on Fig. 3(a) are approximately in good agreement with the X-ray diffraction[28]. ZnO Wurtsite structure structure is identified by one band at 345 cm^{-1}.[27] The bands (144 (E_g)-197(E_g) -399(B_{1g})-519 (B_{1g}) represent the vibrational modes, which are active in spectroscopy of anatase phase of TiO_2.[28-32] and rutile has two raman active modes detected at 447 cm^{-1} 612 cm^{-1} A_{1g}.[27]

At 900°C [Fig. 3(b)] in three ratio molars $ZnTiO_3$ rhomboedral structure is identified by six raman bands at (177-231-266-344-468-709) cm^{-1}.[28] The position of bands of $ZnTiO_3$ as shown on Fig. 3(b) disappearance the peaks of TiO_2 anatase phase in three ratio molars and appearence one peak of rutile raman active mode at 612 cm^{-1} (A_{1g}) confirm the anatase to rutile transformation. A small peaks corresponding to (Eg) 144 cm^{-1} - (B_{1g}) 399 cm^{-1} mode indicating the presence of anatase phase. In our work, it was found that the formation of the rhombohedral phase of $ZnTiO_3$ was obtained at 600°C. However in other works, reaction between the oxides begins at 750°C whereas at 900°C the structure crystallization[28].

The photoluminescence spectrum Fig. 4 (a-b) of two ratio molars Zn/Ti = 0.26 and Zn/Ti = 0.80 calcined at 600°C and 900°C were chosen to study the effect of the percentage of Ti and the increase of the calcination temperature on the optical properties of $ZnTiO_3$ nanobelts. At 600°C, when Zn/Ti = 0.26 [Fig. 4(a)], there is an appearance of one emission band at 526 nm green region. However when the percentage of Ti decreases Zn/Ti = 0.80, one emission band appears at 475 nm blue region. At 900°C [Fig. 4(b)], Zn/Ti = 0.26 three bands appear: 470 nm blue region, 560 nm green region and 800 IR region.

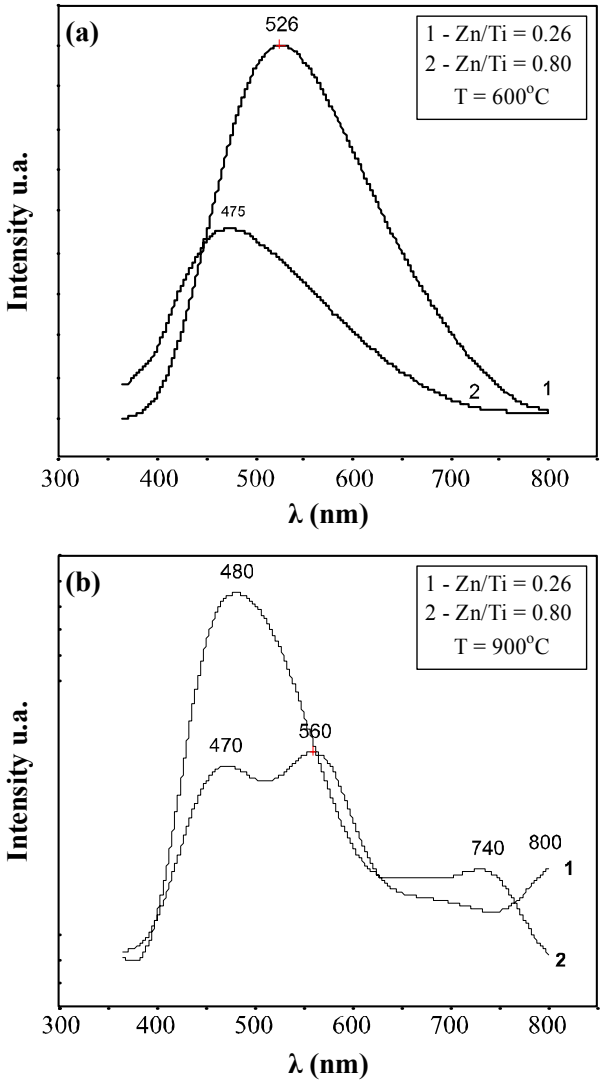

Fig. 4: (a) Photoluminescence of $ZnTiO_3$ of different molar ratios zinc titanate $ZnTiO_3$ nanobelts annealed at 600°C. (b) Photoluminescence of $ZnTiO_3$ of different ratio molars zinc titanate $ZnTiO_3$ nanobelts annealed at 900°C

When Zn/Ti = 0.80, two emission bands appear: 480 nm blue region and 740 nm red region. Table 2 shows that the increase of Ti causes a shift from emitted band to greater wavelengths while the increase of temperature causes a shift from emission bands to greater wavelengths and regeneration of other bands. The emission bands: blue, green, red (visible region) and IR are related to the following structural defects: Oxygen vacancy Vo (hole trapes), Ti^{+3} Interstitials (electron trapes), Zinc vacancy (V_{Zn}) and Intertitial zinc (Zn_i)[33,34].

Table 2: Pholuminescence data showing the wavelengths of emission bands of $ZnTiO_3$ of different molar ratios annealed at 600°C and 900°C

Temperature (°C)	Molar ratio Zn/Ti	λ (nm)	Color region
600°C	0.26	526	Green
	0.80	475	Blue
900°C	0.26	470	Blue
		560	Green
		800	IR
	0.80	480	Blue
		740	Red

CONCLUSION

In this paper, nanobelts of zinc titanate ($ZnTiO_3$) with three ratio molars were produced using electrospinning method. The structure of the pure phase obtained at 600°C is rhombohedral. It is determined by XRD and confirmed by Raman spectroscopy. The Zn_2TiO_4 structure appears at 600°C when Zn/Ti = 0.40 and disappears at 900°C, which was found different of literature. The increase of percentage of titanium in $ZnTiO_3$ favors a shift from emitted bands to greater wavelengths (visible region). However; high temperature causes a shift from emission bands to greater wavelengths and regeneration of other bands. In conclusion, that the increase of Ti rates and the calcination temperatures have useful effect on the optical features of zinc titanate 1D nanostructures.

REFERENCES

1. H. Hafez, Z. Lan and Q. Li, Highly Efficient Dye-sensitized Solar Cells Based on Single Crystalline TiO_2 Nanorod Film, Chem. Lett., **34**, 1506-1507 (2005).
2. K. Fujihara, A. Kumar, R. Jose and S. Ramakrishna, Spray Deposition of Electrospun TiO_2 Nanorods for Dye-sensitized Solar Cell Nanotechnology, **18**, 365709 (2007).
3. R. Sahay, P. Suresh Kumar, R. Sridhar, J. Sundaramurthy, J. Venugopal and S. Ramakrishna, Electrospun Composite Nanofibers and their Multifaceted Applications, J. Mater. Chem., **22**, 12953-12971 (2012).

4. D. Slocombe, A. Porch and M. Pepper, The Mott Transition and Optimal Performance of Transparent Conducting Oxides in Thin Film Solar Cells, Energy and Environ. Sci., **5**, 5387-5391 (2012).

5. C. Guillén and J. Herrero, TCO/metal/TCO Structures for Energy and Flexible Electronics, Thin Solid Films., **520**, 1-17 (2011).

6. J. Watthanaarun, V. Pavarajarn and P. Supaphol, Titanium (IV) Oxide Nanofibers by Combined Sol–gel and Electrospinning Techniques: Preliminary Report on Effects of Preparation Conditions and Secondary Metal Dopant Sci. Tehnol. Adv. Mater., **6**, 240-245 (2005).

7. Y. Tea, C. Matthew Neeves, Q. Smithwick, F. Placido and D. Chu, High Optical and Switching Performance Electrochromic Devices Based on a Zinc Oxide Nanowire with Poly(methyl Methacrylate) Gel Electrolytes, Appl. Phys. Lett., 105 (2014).

8. J.-Y. Park and I.-H. Lee, Photocatalytic Degradation of 2-Chlorophenol using Ag-Doped TiO_2 Nanofibers and a Near-UV Light-Emitting Diode System**,** Inorg. Chem. Commun., **7**, 679-682 (2004).

9. Se Hun Park, B. Park and P. Keun Song, Characteristics of Al-Doped, Ga-Doped and In-Doped Zinc-Oxide Films as Transparent Conducting Electrodes in Organic Light-Emitting Diodes, Curr. Appl. Phys., **10**, S488-S490 (2010).

10. J. Hu, T. Wang Odom and C. M. Lieber, Chemistry and Physics in One Dimension: Synthesis and Properties of Nanowires and Nanotubes, Acc. Chem. Res., **32**, 435-445 (1999).

11. X. Duan, Yu. Huang, Yi. Cui, J. Wang and C. M. Lieber, Indium Phosphide Nanowires as Building Blocks for Nanoscale Electronic and Optoelectronic Devices Nature, **409**, 66-69 (2001).

12. H. Dai, Carbon Nanotube Opportunities and Challenges Sci., **500**, 218-241 (2002).

13. Yu. Wang and J. J. Santiago-Avilés, Synthesis of Lead Zirconatetitanate Nanofibres and the Fourier-transform Infrared Characterization of their Metallo-Organic Decomposition Process Nanotechnology, **15**, 32 (2004).

14. Y. W. Wang, L. D. Zhang, G. Z. Wang, X. S. Peng, Z. Q. Chu and C. H. Liang, Catalytic Growth of Semiconducting Zinc Oxide Nanowires and their Photoluminescence Properties Grawth, **234**, 171-175 (2002).

15. J. Zhang, L. Sun, H. Pan, C. Liao and C. Yan, ZnO Nanowires Fabricated by a Convenient Route, New J. Chem., **26**, 33-34 (2002).

16. Z. Cai , J. Song, J. Li, F. Zhao, X. Luo and X. Tang, Synthesis and Characterization of Zinc Titanate Fibers by Sol-Electrospinning Method, J. Sol-Gel Sci. Technol., **61**, 49-55 (2012).

17. H. Wu, D. Lin, R. Zhang and W. Pan, ZnO Nanofiber Field-Effect Transistor Assembled by Electrospinning, J. Am. Ceram. Soc., **91**, 656-659 (2008).

18. J. Park, J. Moon, S. Lee, S. Lim and T. Zyung, Fabrication and Characterization of ZnO Nanofibers by Electrospinning, Curr. Appl. Phys., **9**, S210-S212 (2009).

19. S.-W. Choi, J. Y. Park and S. S. Kim, Synthesis of SnO_2–ZnO Core–Shell Nanofibers Via a Novel Two-Step Process and their Gas Sensing Properties Nanotechnology, **20**, 465603-455608 (2009).

20. H. Wu, R. Zhang, X. Liu, D. Lin and W. Pan, Electrospinning of Fe, Co and Ni Nanofibers, Synthesis, Assembly and Magnetic Proprieties, Chem. Mater., **19**, 3506-3511 (2007).

21. C. J. Thompson, G. G. Chase, A. L. Yarin and D. H. Reneker, Effects of Parameters on Nanofiber Diameter Determined from Electrospinning Model Polymer, **48**, 6913-6922 (2007).

22. Y. Cheng, W. Huang, Y. Zhang et al., Preparation of TiO_2 Hollow Nanofibers by Electrospining Combined with Sol–gel Process, Cryst. Eng. Comm., **12**, 2256-2260 (2010).

23. A. Chaaya, R. Vviter, M. Bechelany, Z. Alute, D. Erts, A. Zallesskaya, K. Kovalevski, V. Rouessac, V. Smyntyna and P. Miele, Evolution of Microstructure and Related Optical Properties of ZnO Grown by Atomic Layer Deposition, Beilstein J. Nanotechnol., **4**, 690-698 (2013).

24. N. Obradović, N. Labus, T. Srećković, D. Minić and M. Ristić, Synthesis and Characterization of Zinc Titanate Nano-crystal Powders Obtained by Mechanical Activation Science of Sintering, **37**, 123-129 (2005).

25. H. L, H. Y, Z. M. et al., Formation and Transformation of $ZnTiO_3$ Prepared by Sol-Gel Process Mater. Lett., **59**, 197-200 (2005).

26. Z. Dai, K. Liu, Y. Tang, X. Yang, J. Bao and J. Shen, A Novel Tetragonal Pyramid-Shaped Porous ZnO Nanostructure and its Application in the Biosensing of Horseradish Peroxidase, J. Mater. Chem., **18**, 1919-1926 (2008).

27. I. Bobowska, A. Opasin´ska, A. Wypych and P. Wojciechowski, Synthesis and Dielectric Investigations of $ZnTiO_3$ Obtained by a Softchemistry Route, Mater. Chem. Phys., **134**, 87-92 (2012).

28. Y. H. Zhang, C. K. Chan, J. F. Porter and W. Guo, Micro-Raman Spectroscopic Characterization of Nano Sized TiO_2 Powders Prepared by J. Mater. Res., **13**, 2602-2609 (1998).

29. H. C. Choi, Y. M. Jung and S. B. Kim, Size Effects in the Raman Spectra of TiO_2 Nanoparticles, Vibrational Spectroscopy, **37**, 33-38 (2005).

30. S. Balaji, Y. Djaoued and J. Robichaud, Phonon Confinement Studies in Monocrystalline Anatase-TiO_2 Thin Films by Micro Raman Spectroscopy, J. Raman Spectroscopy, **37**, 1416-1422 (2006).

31. Catherine Pighini, Nanocrystal Synthesis of TiO_2 Anatase to Size Distribution Controlled, Influence of the Size of Crystallites on the Raman Spectrum and Study of Properties Surface. Thesis from the University of Burgundy Mention Sciences, Specialty Chemical Physics (2006).

32. L. M. Jeanne and J. K. Fritz, Photoluminescence and Carrier Transport in Nanocrystalline TiO_2, in : Handbook of Luminescent Semi-conducteur Materials, CRC Press (2011) pp. 365-390.

33. C. Ye, Y. Wang, Y. Ye, J. Zhang and G. H. Li, Preparation and Photoluminescence of Undoped $ZnTiO_3$ thin films J. Appl. Phys., **106**, 033520 (2009).

Revised : 28.01.2016 *Accepted : 31.01.2016*